

## Synthesis and characterization of $\text{NdBaMn}_{1.5-x}\text{Co}_{0.5}\text{Nb}_x\text{O}_{5+\delta}$ ( $x=0, 0.1, 0.2$ ) as cathode materials for IT-SOFCs

Xin Kong<sup>1,2</sup>, Shaoping Feng<sup>1,2</sup>, Hongyan Sun<sup>1,2</sup>, Zhongzhou Yi<sup>1,2</sup>, Guiyang Liu<sup>1,2,\*</sup>

<sup>1</sup> Local Characteristic Resource Utilization and New Materials Key Laboratory of Universities in Yunnan, Honghe University, Mengzi 661199, Yunnan, China.

<sup>2</sup> Lab of New Materials for Power Sources, College of Science, Honghe University, Mengzi 661199, Yunnan, China

\*E-mail: [liuguiyang@tsinghua.org.cn](mailto:liuguiyang@tsinghua.org.cn)

Received: 4 June 2018 / Accepted: 4 July 2018 / Published: 5 August 2018

The effect of Nb substitution on structural characteristics, thermal expansion behavior, electrical properties and catalytic activity for oxygen reduction reaction (ORR) of the layered perovskite oxides  $\text{NdBaMn}_{1.5-x}\text{Co}_{0.5}\text{Nb}_x\text{O}_{5+\delta}$  ( $x=0, 0.1, 0.2$ ) has been investigated. After doping with Nb at B-site, the thermal expansion coefficient (TEC) value of  $\text{NdBaMn}_{1.5-x}\text{Co}_{0.5}\text{Nb}_x\text{O}_{5+\delta}$  increases slightly. The average TEC of  $\text{NdBaMn}_{1.5}\text{Co}_{0.5}\text{O}_{5+\delta}$ ,  $\text{NdBaMn}_{1.4}\text{Co}_{0.5}\text{Nb}_{0.1}\text{O}_{5+\delta}$  and  $\text{NdBaMn}_{1.4}\text{Co}_{0.5}\text{Nb}_{0.2}\text{O}_{5+\delta}$  are  $12.89 \times 10^{-6} \text{K}^{-1}$ ,  $13.55 \times 10^{-6} \text{K}^{-1}$  and  $13.38 \times 10^{-6} \text{K}^{-1}$ , respectively, which are much lower than that of Co-based layered perovskites. The electrical conductivity of  $\text{NdBaMn}_{1.5-x}\text{Co}_{0.5}\text{Nb}_x\text{O}_{5+\delta}$  ( $x=0, 0.1, 0.2$ ) samples decrease slightly with Nb content increasing due to the reduction of charge carriers. The doping of Nb greatly benefits the catalytic activity for oxygen reduction reaction. The adsorption/desorption of the molecular oxygen, bulk or surface oxygen diffusion processes during the ORR are improved by Nb doping. The  $R_p$  of  $\text{NdBaMn}_{1.4}\text{Co}_{0.5}\text{Nb}_{0.2}\text{O}_{5+\delta}$  is  $0.07 \Omega\text{cm}^2$  at  $800^\circ\text{C}$  which is triple lower than that of  $\text{NdBaMn}_{1.5}\text{Co}_{0.5}\text{O}_{5+\delta}$  ( $0.21 \Omega\text{cm}^2$  at  $800^\circ\text{C}$ ).  $\text{NdBaMn}_{1.4}\text{Co}_{0.5}\text{Nb}_{0.1}\text{O}_{5+\delta}$  and  $\text{NdBaMn}_{1.4}\text{Co}_{0.5}\text{Nb}_{0.2}\text{O}_{5+\delta}$  samples exhibit low thermal expansion and high catalytic activity as promising cathode materials for IT-SOFCs.

**Keywords:** IT-SOFCs; cathode; Nb doping ; electrochemical performance.

### 1. INTRODUCTION

Solid oxide fuel cells (SOFCs) are promising sustainable energy systems because of their clean energy conversion and high energy efficiency[1]. SOFCs technology could solve the severe consequences of pollution and global warming hopefully. The high operating temperature (above  $1000^\circ\text{C}$ ) is one of the greatest obstacles faced in the large-scale development of this technology[2]. The serious interface reaction between electrode and electrolyte in high operating temperature may

lead to the degradation of electrochemical properties. Besides, expensive materials for interconnects are required in high operating temperature [2, 3]. It's necessary to reduce operating temperature from high temperature to intermediate temperature (500°C-800°C). However, lowering the temperatures to the intermediate ranges lead to a sluggish oxygen reduction reaction (ORR) of cathodes[4, 5]. Hence, a number of researchers make great efforts to develop new mixed ionic and electronic conducting (MIEC) oxides with high catalytic activity as IT-SOFCs electrode materials.

Perovskite oxides include simple perovskite  $ABO_{3-\delta}$  and layered perovskite  $AA'B_2O_{5+\delta}$ . They are promising classes of SOFCs cathode materials[2, 4, 6-10]. Layered perovskite  $AA'B_2O_{5+\delta}$  are A-site ordered and consist of a stacked sequence of  $[AO_\delta]$ - $[BO_2]$ - $[A'O]$ - $[BO_2]$  layers along the c-axis. A is a lanthanide, A' is an alkaline earth element, and B is a transition metal[2, 11]. Such structures enhance the oxygen transport ability and have excellent surface exchange coefficient  $K$  and the chemical diffusion coefficient  $D$  which are much higher than that of simple perovskite  $ABO_{3-\delta}$ [12, 13]. Among the layered perovskite, Cobalt-based  $LnBaCo_2O_{5+\delta}$  (Ln=lanthanide) have received great attention because of their high electronic conductivity and highest oxygen mobility resulting from a high concentration of oxygen vacancies[11, 14-17]. However, similar with other cobalt-based oxides,  $LnBaCo_2O_{5+\delta}$  suffer high thermal expansion properties which not match the electrolyte[1, 18]. It's one of great obstacles faced in the large-scale application as SOFC cathodes.

Cobalt-free layered perovskite such as copper-based layered perovskite [18] or iron-based layered perovskite [19] or Manganese-based layered perovskite[5] have low thermal expansion coefficient(TEC) due to the absence of  $Co^{3+}$  transition from low-spin to high-spin with temperature[3-5]. The TEC value of  $SmBaCu_2O_{5+\delta}$  and  $SmBaCo_{0.4}Mn_{1.5}Mg_{0.1}O_{5+\delta}$  are  $14.6 \times 10^{-6} K^{-1}$  and  $12.58 \times 10^{-6} K^{-1}$ [5, 18]. However, their electrochemical performance are not as good as Cobalt-based layered perovskite [3-5]. Doping at either the A-site[20], B-site [3, 21], or both[22, 23]are effective methods to enhance the electrochemical performance. The doping high valence Nb in perovskite oxide have been investigated[2, 7, 24]. Nb containing perovskite oxide effectively stabilizes the perovskite structure[2] and improved the electrochemical performance[25]. However, Nb doping at B-site in Manganese-based layered perovskite cathodes have not been reported so far. Owing to the potentially effects on the performances of Manganese-based layered perovskite, we systematically investigated the Nb doping into  $NdBaMn_{1.5-x}Co_{0.5}O_{5+\delta}$ . The effect of Nb doping at B-site on structural characteristics, thermal expansion behavior, electrical properties and electrochemical performances of  $NdBaMn_{1.5-x}Co_{0.5}Nb_xO_{5+\delta}$  ( $x=0, 0.1, 0.2$ ) are investigated.

## 2. EXPERIMENTAL

The  $NdBaMn_{1.5-x}Co_{0.5}Nb_xO_{5+\delta}$  ( $x=0, 0.1, 0.2$ ) perovskite oxides were synthesized via sol-gel technique. EDTA and citric acid were complexing agents and dissolved in deionized water at 80°C water bath. Then the required amounts of Nitrates  $Nd(NO_3)_3 \cdot 6H_2O$ ,  $Ba(NO_3)_2$ ,  $Mn(NO_3)_2$ ,  $Co(NO_3)_2 \cdot 6H_2O$  and Niobium oxalate were added. The mole ratio of EDTA and citric acid to the total metal ions was 1:1.5:1. Assistant reagent  $NH_3 \cdot H_2O$  or  $HNO_3$  was added to adjust the pH value to ~6-7. The solution was stirred in water bath for a certain time to form the gel. And the gel was dried in

drying oven to obtain precursors. Then the precursors were sintered in air at 1100°C and 1150°C respectively for 10h to obtain the cathode powders.

The electrolyte powder of  $\text{Sm}_{0.2}\text{Ce}_{0.8}\text{O}_{2-\delta}$  (SDC) was synthesized by the conventional solid reaction method. Required amounts of  $\text{Sm}_2\text{O}_3$  and  $\text{CeO}_2$  were thoroughly mixed using ball-milling and calcined in air at 1200°C for 5 h. The calcined powders with PVA agglomerant were then pressed into disks. Then disks were sintered at 1450°C for 2h to obtain SDC electrolyte.

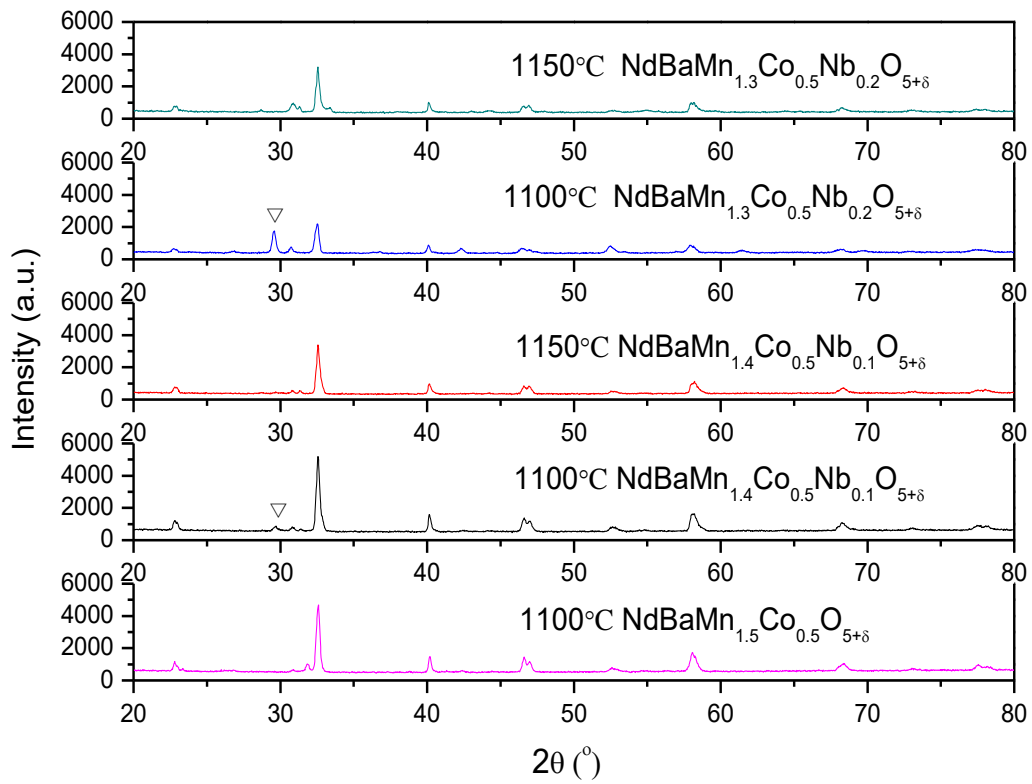
The as-prepared  $\text{NdBaMn}_{1.5-x}\text{Co}_{0.5}\text{Nb}_x\text{O}_{5+\delta}$  ( $x=0, 0.1, 0.2$ ) powders were mixed with organic binders ethylcellulose and terpinol in appropriate ratio to form the cathode slurries and then the slurries applied onto both sides of dense SDC disks. One side with circle pattern was working electrode (WE) and the opposite side with same surface area was counter electrode (CE). The disks were sintered at 1000°C for 2h in air. Current collectors silver pastes were further coated onto the surfaces of electrodes. The disks were sintered at 700°C for 30 minutes in air to form symmetrical cells for the electrochemical performance measurement. The  $\text{NdBaMn}_{1.5-x}\text{Co}_{0.5}\text{Nb}_x\text{O}_{5+\delta}$  ( $x=0, 0.1, 0.2$ ) powders mixed PVA agglomerant evenly were pressed into cuboid samples and heated at 1150°C, 1200°C, 1250°C for 2h to form dense samples to measure the electrical conductivities and TEC.

The synthesized cathodes  $\text{NdBaMn}_{1.5-x}\text{Co}_{0.5}\text{Nb}_x\text{O}_{5+\delta}$  ( $x=0, 0.1, 0.2$ ) were characterized by X-ray diffraction (XRD) using PANalytical X'Pert Powder X-ray Diffractometer. The electrical conductivities of  $\text{NdBaMn}_{1.5-x}\text{Co}_{0.5}\text{Nb}_x\text{O}_{5+\delta}$  ( $x=0, 0.1, 0.2$ ) samples were measured by four-probe dc method from 50°C to 800°C using ST-2258C four point probes meter. The TEC of  $\text{NdBaMn}_{1.5-x}\text{Co}_{0.5}\text{Nb}_x\text{O}_{5+\delta}$  ( $x=0, 0.1, 0.2$ ) were measured by ZRPY-1000 thermal dilatometer from room temperature to 800°C with a heating rate of 5°C/min. The electrochemical performance of  $\text{NdBaMn}_{1.5-x}\text{Co}_{0.5}\text{Nb}_x\text{O}_{5+\delta}$  ( $x=0, 0.1, 0.2$ ) cathodes were measured at different temperatures by ac-impedance spectroscopy using an electrochemical workstation CHI604D from 0.1 Hz to  $10^5$  Hz with the amplitude potential of 10 mV. The electrochemical impedance data were analyzed by the ZSimpWin software.

### 3. RESULTS AND DISCUSSION

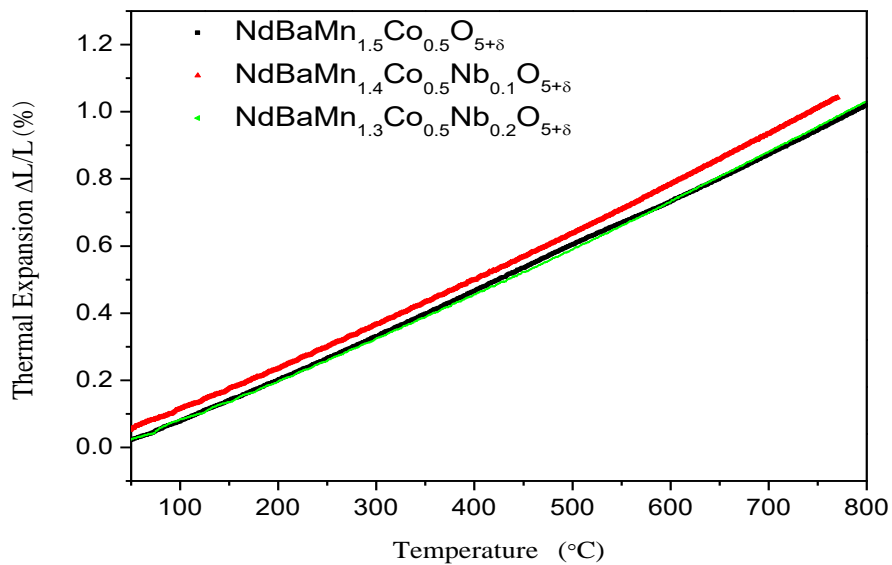
#### 3.1 XRD analysis

The X-ray diffraction patterns of  $\text{NdBaMn}_{1.5-x}\text{Co}_{0.5}\text{Nb}_x\text{O}_{5+\delta}$  ( $x=0, 0.1, 0.2$ ) are shown in Fig.1. The characteristic peaks of  $\text{NdBaMn}_{1.5-x}\text{Co}_{0.5}\text{Nb}_x\text{O}_{5+\delta}$  ( $x=0, 0.1, 0.2$ ) sintered at 1100°C for 10h are layered perovskites[2, 3, 5], but impure peaks at 29.5° are observed in  $\text{NdBaMn}_{1.4}\text{Co}_{0.5}\text{Nb}_{0.1}\text{O}_{5+\delta}$  and  $\text{NdBaMn}_{1.3}\text{Co}_{0.5}\text{Nb}_{0.2}\text{O}_{5+\delta}$ , respectively. When the sintering temperature increases to 1150°C, the impure peaks of  $\text{NdBaMn}_{1.4}\text{Co}_{0.5}\text{Nb}_{0.1}\text{O}_{5+\delta}$  and  $\text{NdBaMn}_{1.3}\text{Co}_{0.5}\text{Nb}_{0.2}\text{O}_{5+\delta}$  disappear which indicates the best sintering temperature of  $\text{NdBaMn}_{1.5-x}\text{Co}_{0.5-x}\text{Nb}_x\text{O}_{5+\delta}$  ( $x=0.1, 0.2$ ) is 1150°C. Partially doping higher valence transition metal cations Nb leads to the increase of sintering temperature of  $\text{NdBaMn}_{1.5-x}\text{Co}_{0.5}\text{Nb}_x\text{O}_{5+\delta}$ .



**Figure 1.** The X-ray diffraction patterns of  $\text{NdBaMn}_{1.5-x}\text{Co}_{0.5}\text{Nb}_x\text{O}_{5+\delta}$  ( $x=0, 0.1, 0.2$ )

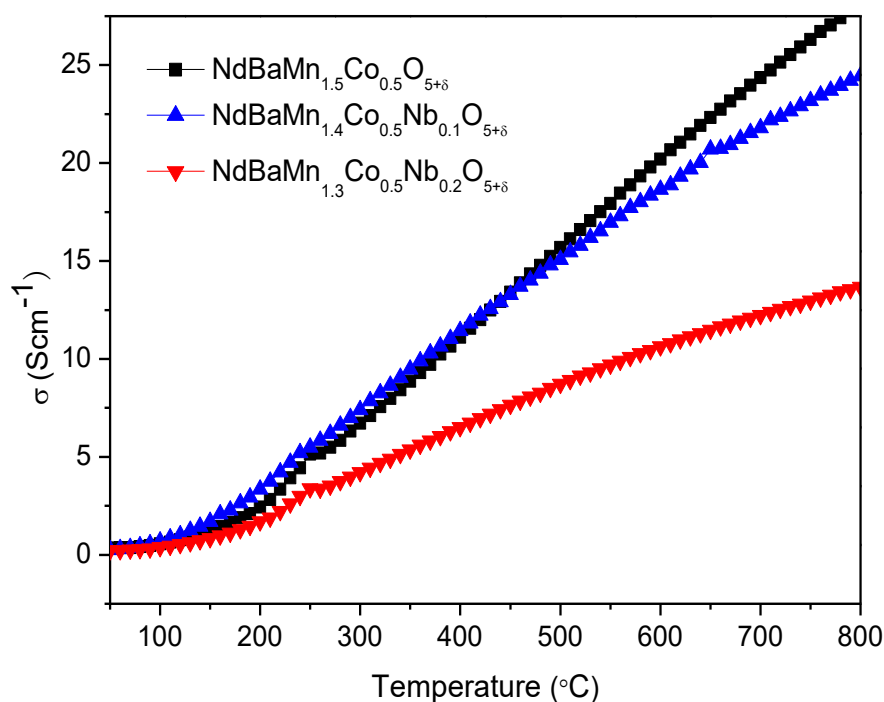
### 3.2 Thermal expansion behavior



**Figure 2.** The thermal-expansion ( $\Delta L/L_0$ ) curves of  $\text{NdBaMn}_{1.5-x}\text{Co}_{0.5}\text{Nb}_x\text{O}_{5+\delta}$  ( $x=0, 0.1, 0.2$ ) from room temperature to 800°C.

The thermal-expansion ( $\Delta L/L_0$ ) curves of  $\text{NdBaMn}_{1.5-x}\text{Co}_{0.5}\text{Nb}_x\text{O}_{5+\delta}$  ( $x=0, 0.1, 0.2$ ) from room temperature to 800 °C are shown in Fig.2. The  $\Delta L/L_0$  is not exactly linear dependent on temperature, the slope of the thermal expansion curves increases with temperature increasing due to oxygen loss and the consequent reduction of the (Mn, Co and Nb) ions[4, 26]. The average TEC of  $\text{NdBaMn}_{1.5}\text{Co}_{0.5}\text{O}_{5+\delta}$ ,  $\text{NdBaMn}_{1.4}\text{Co}_{0.5}\text{Nb}_{0.1}\text{O}_{5+\delta}$  and  $\text{NdBaMn}_{1.3}\text{Co}_{0.5}\text{Nb}_{0.2}\text{O}_{5+\delta}$  are  $12.89 \times 10^{-6} \text{K}^{-1}$ ,  $13.55 \times 10^{-6} \text{K}^{-1}$  and  $13.38 \times 10^{-6} \text{K}^{-1}$ , respectively. The thermal expansion behavior of layered perovskite oxides is mainly caused by chemical expansion related to reduction of B-site transition metal ions to lower oxidation states and their spin transition [4, 7]. The chemical expansion in  $\text{NdBaMn}_{1.5-x}\text{Co}_{0.5}\text{Nb}_x\text{O}_{5+\delta}$  is mainly caused by the reduction of (Mn, Co and Nb) ions and the cobalt spin transition. The ionic radius of  $\text{Co}^{3+}$  (0.055 nm for low spin and 0.061 nm for high spin),  $\text{Mn}^{3+}$  (0.058 nm for low spin and 0.065 nm for high spin) and  $\text{Nb}^{3+}$  (0.072 nm) is larger than  $\text{Co}^{4+}$  (0.053 nm),  $\text{Mn}^{4+}$  (0.053 nm) and  $\text{Nb}^{5+}$  (0.064 nm), respectively. After doping with Nb at B-site, the TEC value of  $\text{NdBaMn}_{1.5-x}\text{Co}_{0.5}\text{Nb}_x\text{O}_{5+\delta}$  increases slightly. However, the TECs of all the  $\text{NdBaMn}_{1.5-x}\text{Co}_{0.5}\text{Nb}_x\text{O}_{5+\delta}$  samples are ~35% lower than that of Co-based layered perovskites, such as  $\text{NdBaCo}_2\text{O}_{5+\delta}$  ( $21.0 \times 10^{-6} \text{K}^{-1}$ )[10],  $\text{NdBa}_{0.5}\text{Sr}_{0.5}\text{Co}_2\text{O}_{5+\delta}$  ( $20.27 \times 10^{-6} \text{K}^{-1}$ ) [10]. The TECs of  $\text{NdBaMn}_{1.5-x}\text{Co}_{0.5}\text{Nb}_x\text{O}_{5+\delta}$  are more compatible with that of SDC electrolyte ( $12.20 \times 10^{-6} \text{K}^{-1}$ [10]) which could enhance the long-term stability of  $\text{NdBaMn}_{1.5-x}\text{Co}_{0.5}\text{Nb}_x\text{O}_{5+\delta}$ .

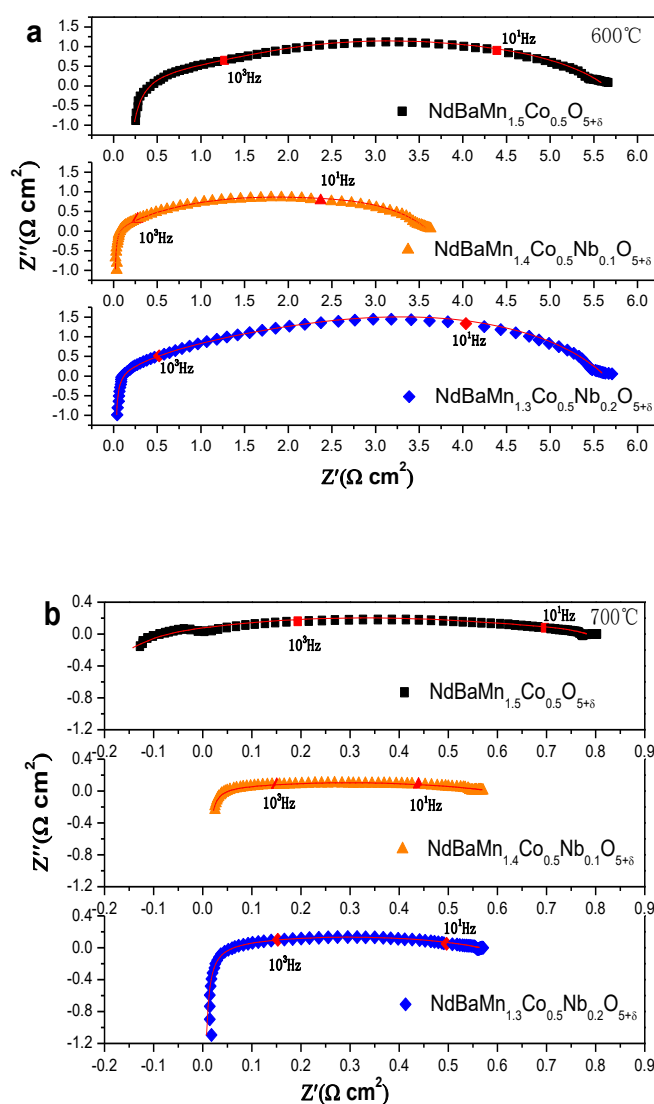
### 3.3 Electrical conductivity



**Figure 3.** The electrical conductivity of  $\text{NdBaMn}_{1.5-x}\text{Co}_{0.5}\text{Nb}_x\text{O}_{5+\delta}$  ( $x=0, 0.1, 0.2$ ) from 50 °C to 800 °C in air.

The temperature dependence of electrical conductivity of  $\text{NdBaMn}_{1.5-x}\text{Co}_{0.5}\text{Nb}_x\text{O}_{5+\delta}$  ( $x=0, 0.1, 0.2$ ) samples from 50 °C to 800 °C in air are shown in Fig.3. The conductivity of  $\text{NdBaMn}_{1.5-x}\text{Co}_{0.5}\text{Nb}_x\text{O}_{5+\delta}$  ( $x=0, 0.1, 0.2$ ) increases gradually with temperature increasing and shows a typical semiconductor behavior which is similar to cobalt layered perovskites oxides  $\text{NdBaCo}_2\text{O}_{5+\delta}$ [26]. The increased electrical conductivity with temperature can be ascribed to thermal-activation of electronic hopping[4]. The maximum conductivity of  $\text{NdBaMn}_{1.5-x}\text{Co}_{0.5}\text{Nb}_x\text{O}_{5+\delta}$  ( $x=0, 0.1, 0.2$ ) is  $28.14 \text{ Scm}^{-1}$ ,  $24.45 \text{ Scm}^{-1}$  and  $13.66 \text{ Scm}^{-1}$  at 800°C, respectively. The conductivity decreases with Nb content due to the stronger Nb-O bond (753 kJ/mol) compared with Mn-O bond (360 kJ/mol) and Co-O bond (368 kJ/mol)[2]. The strong Nb-O bond leads to the charge carriers decrease which related to the decrease in the electron cloud overlap between the (Co, Mn):3d orbital and O:2p orbital [5, 27].

### 3.4 Electrochemical properties



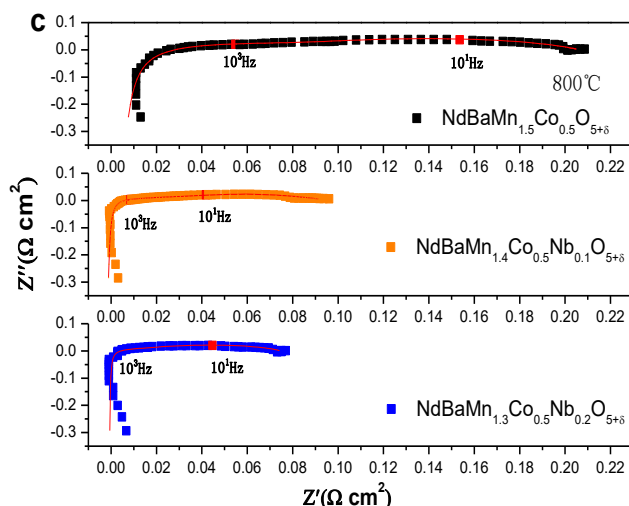


**Figure 4.** Experimental and fitting Nyquist impedance spectra of  $\text{NdBaMn}_{1.5-x}\text{Co}_{0.5}\text{Nb}_x\text{O}_{5+\delta}$  ( $x=0, 0.1, 0.2$ ) cathodes at (a) 600 °C, (b) 700 °C and (c) 800 °C in air.

The electrochemical performances of the  $\text{NdBaMn}_{1.5-x}\text{Co}_{0.5}\text{Nb}_x\text{O}_{5+\delta}$  ( $x=0, 0.1, 0.2$ ) cathodes toward ORR are tested on symmetrical cells NBMCNO/SDC/ NBMCNO by means of EIS. Fig4a-c show the experimental and fitting Nyquist impedance spectra of  $\text{NdBaMn}_{1.5-x}\text{Co}_{0.5}\text{Nb}_x\text{O}_{5+\delta}$  ( $x=0, 0.1, 0.2$ ) cathodes at (a) 600 °C, (b) 700 °C and (c) 800 °C in air. In order to investigate the process of ORR of  $\text{NdBaMn}_{1.5-x}\text{Co}_{0.5}\text{Nb}_x\text{O}_{5+\delta}$  ( $x=0, 0.1, 0.2$ ), the impedance spectra are analyzed by fitting equivalent circuit models using ZSimpWin software. Table 1-3 list the EIS fitting results of  $\text{NdBaMn}_{1.5-x}\text{Co}_{0.5}\text{Nb}_x\text{O}_{5+\delta}$  ( $x=0, 0.1, 0.2$ ) cathode measured in air. The corresponding fitting equivalent circuit models for different samples at different temperature also list in Tables. The  $R_{el}$  at high frequency represents the ohmic resistance which includes the resistance contributions of the electrolyte, the electrodes, the current collectors and the lead wires. The  $R_{el}$  of  $\text{NdBaMn}_{1.5-x}\text{Co}_{0.5}\text{Nb}_x\text{O}_{5+\delta}$  ( $x=0, 0.1, 0.2$ ) is subtracted to facilitate the comparison of electrochemical activity of cathodes at different temperatures. L represents a high frequency induction tail ascribed to the device and connects leads; Q represents a nonideal capacitor;  $R_1$ ,  $R_2$  and  $R_3$  are related to the high frequency polarization resistances  $R_H$  and low frequency polarization resistance  $R_L$ . The total polarization resistance  $R_p$  is defined by the sum of resistances  $R_H$  and  $R_L$ .  $R_H$  are ascribed to the charge transfer processes[1, 9, 10].  $R_L$  is associated with the adsorption/desorption of the molecular oxygen, bulk or surface oxygen diffusion processes[5]

It can be seen in Table 1, the  $R_3$ (low frequency polarization resistance  $R_L$ ) of  $\text{NdBaMn}_{1.5}\text{Co}_{0.5}\text{O}_{5+\delta}$  is larger than the sum of  $R_1$  and  $R_2$ (high frequency polarization resistances  $R_H$ ), which indicates the oxygen diffusion processes are the rate-determining step of ORR. For  $\text{NdBaMn}_{1.4}\text{Co}_{0.5}\text{Nb}_{0.1}\text{O}_{5+\delta}$  and  $\text{NdBaMn}_{1.4}\text{Co}_{0.5}\text{Nb}_{0.2}\text{O}_{5+\delta}$ , increasing the content of Nb greatly benefits the ORR. At 700 °C and 800 °C,  $R_2$  of  $\text{NdBaMn}_{1.4}\text{Co}_{0.5}\text{Nb}_{0.1}\text{O}_{5+\delta}$  and  $\text{NdBaMn}_{1.4}\text{Co}_{0.5}\text{Nb}_{0.2}\text{O}_{5+\delta}$  dramatically reduces which indicates the adsorption/desorption of the molecular oxygen, bulk or surface oxygen diffusion processes are improved. It may be ascribed to the increase of oxygen vacancy causes by high valence Nb doping at B site.

The  $R_p$  of  $\text{NdBaMn}_{1.4}\text{Co}_{0.5}\text{Nb}_{0.2}\text{O}_{5+\delta}$  is  $0.07\Omega\text{cm}^2$  at  $800^\circ\text{C}$  which is triple lower than that of  $\text{NdBaMn}_{1.5}\text{Co}_{0.5}\text{O}_{5+\delta}$  ( $0.21\Omega\text{cm}^2$  at  $800^\circ\text{C}$ ). The  $R_p$  of  $\text{NdBaMn}_{1.4}\text{Co}_{0.5}\text{Nb}_{0.1}\text{O}_{5+\delta}$  and  $\text{NdBaMn}_{1.4}\text{Co}_{0.5}\text{Nb}_{0.2}\text{O}_{5+\delta}$  are much lower than Manganese-based perovskite  $\text{La}_{0.8}\text{Sr}_{0.2}\text{Co}_{0.17}\text{Mn}_{0.83}\text{O}_{3-\delta}$  ( $2.4\Omega\text{cm}^2$  at  $800^\circ\text{C}$ )[28],  $\text{Sm}_{0.5}\text{Sr}_{0.5}\text{MnO}_3$  ( $1.92\Omega\text{cm}^2$  at  $800^\circ\text{C}$ )[29], and  $\text{PrBaCo}_{1.7}\text{Mn}_{0.3}\text{O}_{5+\delta}$  ( $0.15\Omega\text{cm}^2$  at  $800^\circ\text{C}$ )[4].

**Table 1.** EIS fitting results of  $\text{NdBaMn}_{1.5}\text{Co}_{0.5}\text{O}_{5+\delta}$  cathode measured in air.

T ( $^\circ\text{C}$ )	L ( $\text{Hcm}^2$ )	$R_{el}$ ( $\Omega\text{cm}^2$ )	$R_1$ ( $\Omega\text{cm}^2$ )	$R_2$ ( $\Omega\text{cm}^2$ )	$R_3$ ( $\Omega\text{cm}^2$ )	$R_p$ ( $\Omega\text{cm}^2$ )	Model
600	2.075E-6	17.06	1.72	1.28	2.64	5.64	LR(QR)(QR)(QR)
700	6.501E-7	6.66	0.0001	0.13	0.65	0.78	LR(QR)(QR)(QR)
800	4.875E-7	2.78	9.973E-6	0.11	0.10	0.21	LR(QR)(QR)(QR)

**Table 2.** EIS fitting results of  $\text{NdBaMn}_{1.4}\text{Co}_{0.5}\text{Nb}_{0.1}\text{O}_{5+\delta}$  cathode measured in air.

T ( $^\circ\text{C}$ )	L ( $\text{Hcm}^2$ )	$R_{el}$ ( $\Omega\text{cm}^2$ )	$R_1$ ( $\Omega\text{cm}^2$ )	$R_2$ ( $\Omega\text{cm}^2$ )	$R_p$ ( $\Omega\text{cm}^2$ )	Model
600	1.937E-6	12.54	0.58	3.05	3.63	LR(QR)(QR)
700	4.958E-7	4.17	0.60	-	0.60	LR(QR)
800	5.493E-7	1.75	0.03	0.07	0.10	LR(QR)(QR)

**Table 3.** EIS fitting results of  $\text{NdBaMn}_{1.3}\text{Co}_{0.5}\text{Nb}_{0.2}\text{O}_{5+\delta}$  cathode measured in air.

T ( $^\circ\text{C}$ )	L ( $\text{Hcm}^2$ )	$R_{el}$ ( $\Omega\text{cm}^2$ )	$R_1$ ( $\Omega\text{cm}^2$ )	$R_2$ ( $\Omega\text{cm}^2$ )	$R_p$ ( $\Omega\text{cm}^2$ )	Model
600	1.96E-6	16.56	2.83	2.81	5.64	LR(QR)(QR)
700	2.124E-6	5.76	0.53	0.04	0.57	LR(QR)(QR)
800	5.653E-7	2.45	0.05	0.02	0.07	LR(QR)(QR)

#### 4. CONCLUSIONS

With an aim to develop new cathode materials with lower TEC and adequate electrochemical activity for IT-SOFC, the substitution of Nb at B site of  $\text{NdBaMn}_{1.5-x}\text{Co}_{0.5}\text{Nb}_x\text{O}_{5+\delta}$  ( $x=0, 0.1, 0.2$ ) have been investigated. Although the TEC value of  $\text{NdBaMn}_{1.5-x}\text{Co}_{0.5}\text{Nb}_x\text{O}_{5+\delta}$  increases slightly with Nb substituting, the TEC value is very compatible with that of traditional electrolyte SDC. The electrical conductivity of  $\text{NdBaMn}_{1.5-x}\text{Co}_{0.5}\text{Nb}_x\text{O}_{5+\delta}$  decreases slightly after Nb doping. The electrochemical performances of  $\text{NdBaMn}_{1.5-x}\text{Co}_{0.5}\text{Nb}_x\text{O}_{5+\delta}$  ( $x=0, 0.1, 0.2$ ) are improved owing to the improvement of oxygen diffusion processes. The  $R_p$  of  $\text{NdBaMn}_{1.4}\text{Co}_{0.5}\text{Nb}_{0.1}\text{O}_{5+\delta}$  and  $\text{NdBaMn}_{1.4}\text{Co}_{0.5}\text{Nb}_{0.2}\text{O}_{5+\delta}$  are

$0.10\Omega\text{cm}^2$  and  $0.07\Omega\text{cm}^2$  at  $800^\circ\text{C}$ . The results indicate that the  $\text{NdBaMn}_{1.5-x}\text{Co}_{0.5}\text{Nb}_x\text{O}_{5+\delta}$  ( $x=0, 0.1, 0.2$ ) are promising cathode materials for IT-SOFCs.

#### ACKNOWLEDGEMENTS

This work was supported by the Yunnan Applied Basic Research Project (No.2017FD157), the National Natural Science Foundation of China (No.51662007 and No.U1602273), Yunnan Local Colleges (part) Applied Basic Projects Joint Special Foundation (No.2017FH001-120).

#### References

1. X. Ding, X. Kong, H. Wu, Y. Zhu, J. Tang and Y. Zhong, *Int. J. Hydrogen Energy*, 37 (2012) 2546.
2. M. Saccoccio, C. Jiang, Y. Gao, D. Chen and F. Ciucci, *Int. J. Hydrogen Energy*, 42 (2017) 19204.
3. J. Kim, S. Choi, S. Park, C. Kim, J. Shin and G. Kim, *Electrochim. Acta*, 112 (2013) 712.
4. W. Guo, R. Guo, L. Liu, G. Cai, C. Zhang, C. Wu, Z. Liu and H. Jiang, *Int. J. Hydrogen Energy*, 40 (2015) 12457.
5. X. Kong, H. Sun, Z. Yi, B. Wang, G. Zhang and G. Liu, *Ceram. Int.*, 43 (2017) 13394.
6. J. Wang, K.Y. Lam, M. Saccoccio, Y. Gao, D. Chen and F. Ciucci, *J. Power Sources*, 324 (2016) 224.
7. Z.-B. Yang, M.-F. Han, P. Zhu, F. Zhao and F. Chen, *Int. J. Hydrogen Energy*, 36 (2011) 9162.
8. R.A. De Souza, J.A. Kilner and J.F. Walker, *Mater. Lett.*, 43 (2000) 43.
9. X. Ding, X. Kong, J. Jiang, C. Cui and L. Guo, *Int. J. Hydrogen Energy*, 35 (2010) 1742.
10. X. Kong, G. Liu, Z. Yi and X. Ding, *Int. J. Hydrogen Energy*, 40 (2015) 16477.
11. G. Kim, S. Wang, A.J. Jacobson, L. Reimus, P. Brodersen and C.A. Mims, *J. Mater. Chem.*, 17 (2007) 2500.
12. A.A. Taskin, A.N. Lavrov and Y. Ando, *Phys.*, (2005)
13. C. Chen, D. Chen and F. Ciucci, *Phys. Chem. Chem. Phys.*, 17 (2015) 7831.
14. W. Wang, T.S. Peh, S.H. Chan and T.S. Zhang, *ECS Trans.*, 25 (2009) 2277.
15. A. Chang, S.J. Skinner and J.A. Kilner, *Solid State Ionics*, 177 (2006) 2009.
16. Y. Lee, D.Y. Kim and G.M. Choi, *Solid State Ionics*, 192 (2011) 527.
17. A. Tarancón, A. Morata, G. Dezanneau, S.J. Skinner, J.A. Kilner, S. Estradé, F. Hernández-Ramírez, F. Peiró and J.R. Morante, *J. Power Sources*, 174 (2007) 255.
18. X. Kong and X. Ding, *Int. J. Hydrogen Energy*, 36 (2011) 15715.
19. H. Ding and X. Xue, *J. Power Sources*, 195 (2010) 7038.
20. D. Fu, F. Jin and T. He, *J. Power Sources*, 313 (2016) 134.
21. A. Jun, T.H. Lim, J. Shin and G. Kim, *Int. J. Hydrogen Energy*, 39 (2014) 20791.
22. L. Jiang, T. Wei, R. Zeng, W.-X. Zhang and Y.-H. Huang, *J. Power Sources*, 232 (2013) 279.
23. B. Wang, G. Long, Y. Ji, M. Pang and X. Meng, *J. Alloys Compd.*, 606 (2014) 92.
24. K.T. Lee and A. Manthiram, *Solid State Ionics*, 178 (2007) 995.
25. T. Yu, X. Mao and G. Ma, *J. Alloys Compd.*, 608 (2014) 30.
26. J.H. Kim and A. Manthiram, *Electrochim. Acta*, 54 (2009) 7551.
27. A. Jun, T.-h. Lim, J. Shin and G. Kim, *Int. J. Hydrogen Energy*, 39 (2014) 20791.
28. Y. Bai, M. Liu, D. Ding, K. Blinn, W. Qin, J. Liu and M. Liu, *J. Power Sources*, 205 (2012) 80.
29. W. Li, J. Pu, B. Chi and L. Jian, *Electrochim. Acta*, 141 (2014) 189.